

## Electric field induced tunneling process in the quantum wells

Sudhira Panda<sup>1</sup> and B K Panda<sup>2</sup>

<sup>1</sup>Institute of Mathematics and Applications, Bhubaneswar-751 005, Orissa, India

<sup>2</sup>Institute of Physics, Bhubaneswar-751 005, Orissa, India

E-mail : \*sudhira@iopb.res.in;

**Abstract** : In this study, the field induced direct tunneling and phonon-assisted tunneling of electrons from the single quantum well based on the AlGaAs/GaAs heterojunction are reported. The barrier lowering due to the applied electric field favours electrons to tunnel out of the well. The longitudinal optic phonon at a finite temperature scatters electrons to the continuum and then the electron escapes out of the well in the direction of the electric field. The thermally excited electrons also escape from the well by the thermionic process. The dark current is calculated taking different field induced tunneling mechanisms. The electron absorbs photons and generates photo-current in the direction of the electric field. The magnitude of the photo-current is an order of magnitude higher than the dark current.

**Keywords** Single quantum well, electron tunneling, dark current.

**PACS Nos.** . 73.40.-c, 73.61.Ey, 63.20. Kr

### 1. Introduction

Fabrication of infrared photo-detectors using the semiconductor quantum wells have been rapidly developed. Many experimental and theoretical activities have been carried to optimize efficiency of these devices [1]. The important criterion for achieving efficient devices is that the photo-current of these devices should be an order of magnitude higher than dark current [2]. In order to find the key parameters for improving the device qualities, the modeling of the photo-current and dark current is needed. The calculation of photo-current requires quantum mechanical descriptions of photon-assisted tunneling of electrons in a biased quantum well. On the other hand, the field induced direct tunneling, phonon-assisted tunneling and thermionic emission processes constitute the dark current.

The direct escape rate of electrons through the tilted barrier in the quantum wells by the applied field has been studied using the analytic Airy function approaches [3]. However, these methods are very unstable at low field strength. In the numerical methods, the density of states are

calculated from the stabilization graph and the Stark shifted energies and lifetimes are obtained by fitting a Lorentzian with it [4]. However, compared to the Airy function method this procedure is quite involved and time consuming. We have therefore present a new method for calculating the direct tunneling rate. In this method the density of states are calculated using as arbitrary energy dependent wave function. This method is simple to implement and can be extended to find field induced tunneling in quantum wires and dots.

While the direct escape rate is found to increase exponentially with increasing electric field, the phonon escape rate is important at low fields. The phonon-assisted tunneling constitutes the electron scattering with the longitudinal optic (LO) phonon, longitudinal acoustic phonon and interface LO phonon [5,6]. The electron does not couple with the transverse phonon [7]. The scattering due to the longitudinal optic (LO) phonon is found to be significant over the longitudinal acoustic phonon [8]. The dominant LO phonon-assisted tunneling has been studied before by several groups treating LO phonon as a bulk mode [9–11].

\*Corresponding Author

However, these calculations involve several integrals which need large computational time. In our method we have simplified the integrals and found an expression which needs modest computational time.

In this paper we have studied the average escape rates from different tunneling mechanisms under applied electric fields in a single narrow rectangular QW based on AlGaAs/GaAs heterojunction. This well contains a single bound state. This is because for the detector application the quantum well structure needs a single bound state with excited state close to the barrier height. The field induced tunneling rates are then calculated to find the dark current and it is compared with the photo-current.

## 2. Methods of calculations and results

### 2.1. Direct tunneling :

The Schrödinger equation for a bound state energy  $E_0$  is given by

$$H\Psi_{E_0}(z) = E_0\Psi_{E_0}(z). \quad (1)$$

The Hamiltonian  $H$  in the effective mass equation under applied electric field is given by [12]

$$H = -\frac{\hbar^2}{2} \frac{\partial}{\partial z} \frac{1}{m^*(z)} \frac{\partial}{\partial z} + V(z) + \frac{\hbar^2 k_t^2}{2m^*(z)} + eFz. \quad (2)$$

Here,  $m^*(z)$  is the position dependent effective mass with the well mass  $m_w^*$  and barrier mass  $m_b^*$  which are the effective masses of GaAs and Al<sub>x</sub>Ga<sub>1-x</sub>As respectively.  $V(z)$  is the confinement potential with barrier height  $V_0$ .  $k_t$  is the transverse momentum of the two-dimensional electron gas and  $F$  is the electric field.

The method for finding resonance position  $E_0$  and width  $G$  from the density of states has been formulated by several groups [3,10].

The density of states at an arbitrary energy  $E$  is defined as [3]

$$\rho(E) \left[ \int dz \Psi_E^*(z) \Psi_{E'}(z) \right] = \delta(E - E'). \quad (3)$$

The energy dependent wave function  $\Psi_E(z)$  is reasonably approximated by the Taylor's expansion as

$$\Psi_E(z) = \Psi_{E_0}(z) + (E - E_0) \dot{\Psi}_{E_0}(z), \quad (4)$$

where  $\dot{\Psi}_{E_0}(z)$  is the energy derivative of  $\Psi_E(z)$  at the bound state energy  $E_0$ .

Differentiating eq. (1) with respect to  $E$ , we find  $\dot{\Psi}_{E_0}(z)$  satisfying the equation

$$(H - E_0) \dot{\Psi}_{E_0}(z) = \Psi_{E_0}(z). \quad (5)$$

Naturally  $\Psi_{E_0}(z)$  is normalized as

$$\int \Psi_{E_0}^*(z) \Psi_{E_0}(z) dz = 1. \quad (6)$$

From eqs. (5) and (6) we obtain

$$\int_{-\infty}^{\infty} \Psi_{E_0}^*(z) (H - E_0) \dot{\Psi}_{E_0}(z) dz = 1. \quad (7)$$

The normalization constant for  $\Psi_{E_0}(z)$  is found from this equation. Differentiating eq. (6) with respect to  $E$  at  $E_0$ , we obtain

$$\int_{-\infty}^{\infty} [\dot{\Psi}_{E_0}^*(z) \Psi_{E_0}(z) + \dot{\Psi}_{E_0} \Psi_{E_0}^*(z)] dz = 0. \quad (8)$$

Substituting eq. (4) in eq. (3) and then using eqs. (6) and (8), the density of states is obtained as

$$\rho(E) = \frac{1}{1 + (E - E_0)^2 N} \quad (9)$$

where  $N = \int_{-\infty}^{\infty} |\dot{\Psi}_{E_0}(z)|^2 dz$ .

The exact form of the density of states is usually described by a Lorentzian

$$\rho(E) = \rho(E_0) \frac{(\Gamma/2)^2}{(E - E_0)^2 + (\Gamma/2)^2}. \quad (11)$$

The resonance width  $G$  is obtained by comparing eq. (11) with eq. (9) as

$$\Gamma = \frac{1}{\sqrt{N}} \quad (12)$$

The initial energy including the two-dimensional transverse kinetic energy is given by

$$E_i = E_0 + \frac{\hbar^2 k_t^2}{2m_w^*} \quad (13)$$

The initial energy dependent escape rate due to the direct tunneling is obtained as  $1/\tau_{dt}(E_i) = \Gamma(E_i)/\hbar$ . The escape rate is found by averaging over the initial carrier distributions as

$$\left\langle \frac{1}{\tau_{dt}} \right\rangle = \int dE_{ip}(E_i) f(E_i) \frac{1}{\tau_{dt}(E_i)} / \int dE_{ip}(E_i) f(E_i). \quad (14)$$

The numerical solution of the eq. (1) is based on the Fourier series method [4]. The effect of the artificial triangular potential created in the direction of the applied field is removed by a self-consistent method [4]. The effective masses in the well ( $m_w^*$ ) and barrier ( $m_b^*$ ) regions are  $0.067 m_0$  and  $0.095 m_0$  respectively, where  $m_0$  is the free electron mass. The Al concentration  $x$  is taken as 0.353 which results the barrier height ( $V_0$ ) 340 meV. The width of

the well is taken as 40 Å so that it contains one bound state at energy 170 meV.

The average escape rate due to the direct tunneling is shown in Figure 1.

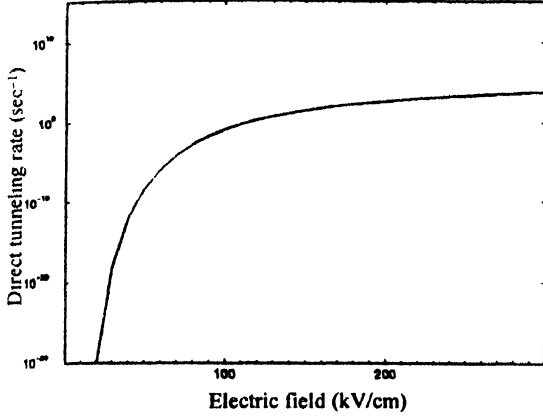


Figure 1. Direct tunneling rate as a function of applied electric field strength.

We find that it increases very rapidly with applied electric field. The behaviour of the escape rate is understood in terms of the semiclassical approximation [13] where it is explained that the rate increases exponentially with the applied electric fields.

## 2.2 Phonon-assisted tunneling :

The escape rate due to the LO phonon as a function of the initial energy is described in the Fermi golden rule as [14]

$$\frac{1}{\tau_{ph}} = \frac{2\pi}{\hbar} \sum_{i,f,q} |M_{fi}(q)|^2 N(\omega_{LO}) [1 - f(E_f)] f(E_i) \times \delta(E_f - E_i - \hbar\omega_{LO}), \quad (15)$$

where  $\hbar\omega_{LO}$  is the energy of the LO phonon,  $N(\omega)$  is the Boson distribution function and  $q$  is the momentum of phonon.  $E_i$  and  $E_f$  are the initial and final states energies respectively. The electron-phonon coupling matrix element  $M_{fi}(q)$  is defined as

$$M_{fi}(q) = \langle \Psi_f(r) | H_{ep}(q) | \Psi_i(r) \rangle. \quad (16)$$

The final energy  $E_f$  is given by

$$E_f = E_i + \frac{\hbar^2 k_f^2}{2m_B^*}. \quad (17)$$

The electron LO phonon interaction expressed in the Frölich form is described as [15]

$$H_{ep}(q) = \sum_q \left[ \frac{\gamma}{q\Omega} \right]^{1/2} e^{-iq \cdot r}, \quad (18)$$

where  $\gamma$  is defined as

$$\gamma = \frac{4e^2 \hbar \omega_{LO}}{\hbar^3} \left( \frac{1}{\epsilon_\infty} - \frac{1}{\epsilon_0} \right) \quad (19)$$

Here,  $\Omega$  is the arbitrary volume of the quantum well. The  $\epsilon_\infty$  and  $\epsilon_0$  are the high frequency and static dielectric constants of GaAs respectively.

Due to the two-dimensional nature of the electron gas in a quantum well, the wave function is described as

$$(r) = \sqrt{\frac{1}{A}} e^{ik_t \cdot r_t} \Psi_{E_a}(z), \quad (20)$$

where  $r_t$  and  $k_t$  are transverse position and momentum respectively.  $A$  is the area of the two-dimensional gas.

The square of the matrix element is derived as

$$|M_{fi}(q)|^2 = \frac{\gamma}{\Omega} \delta_{k_f, k_i + q} \int dq_z \int dq_t \frac{|Z(q_z, E_{k'})|^2}{q_t^2 + q_z^2}, \quad (21)$$

$$\text{where } Z(q_z, E_{k'}) = \int dz \Psi_{E_{k'}}^*(z) e^{-iq_z z} \Psi_{E_0}(z). \quad (22)$$

Combining the energy and momentum conservations in the transverse direction and solving for  $q_t$  we obtain

$$\delta(E_{k_i + q_t} - E_{k_i} - \hbar\omega_{LO}) = \frac{2m_B^*}{\hbar^2} |Q_+ - Q_-| \times [\delta(q_t - Q_+) + \delta(q_t - Q_-)], \quad (23)$$

$$\text{where } Q_\pm = -k_i \cos \theta \pm k_i \sqrt{\cos^2(\theta) - \Delta - 1}. \quad (24)$$

Here,  $\Delta = (E_{k'} - E_0 - \hbar\omega_{LO})/E_i - m_B^*/m_W^*$  and  $E_i = \hbar^2 k_i^2 / 2m_B^*$ . The initial energy dependent escape rate is obtained as

$$\frac{1}{\tau_{ph}(E_i)} = \beta N(\omega_{LO}) [1 - f(E_i + \hbar\omega_{LO})] \int_{E_0}^\infty dE_{k'} P(E_{k'}) \times \int_0^\infty dq_z \Theta(q_z, E_i, E_{k'}) Z(q_z, E_{k'}) \quad (25)$$

where  $\beta = \pi\gamma$ . The expression for  $\Theta(q_z, E_i, E_{k'})$  is given by

$$\Theta(q_z, E_i, E_{k'}) = \int_0^{2\pi} d\theta \frac{1}{|Q_+ - Q_-|} \times \left( \frac{Q_+}{q_z^2 + Q_+^2} + \frac{Q_-}{q_z^2 + Q_-^2} \right). \quad (26)$$

Following the method of Harrison [15], the integration over  $\theta$  is simplified as

$$\Theta(q_z, E_{k'}, E_k) = \pi \left[ q_z^4 + \left( \frac{4m_B^* q_z^2}{\hbar^2} \right) E_i (1 + \Delta) + \left( \frac{2m_B^*}{\hbar^2} \right)^2 E_i^2 (1 - \Delta)^2 \right]^{-1/2}. \quad (27)$$

The rate  $\langle 1/\tau_{ph} \rangle$  is obtained by averaging over the carrier distributions in the initial state as described in eq. (14).

The parameters used in this calculations are :  $\epsilon_\infty = 10.6$ ,  $\epsilon_0 = 12.4$  and  $\hbar\omega_{LO} = 35$  meV. In Figure 2 the phonon-assisted tunneling rates are presented for various temperatures. While the direct tunneling rate increases exponentially with the electric fields, the phonon scattering rate does not change significantly with fields. As expected, the escape rates are highly temperature dependent.

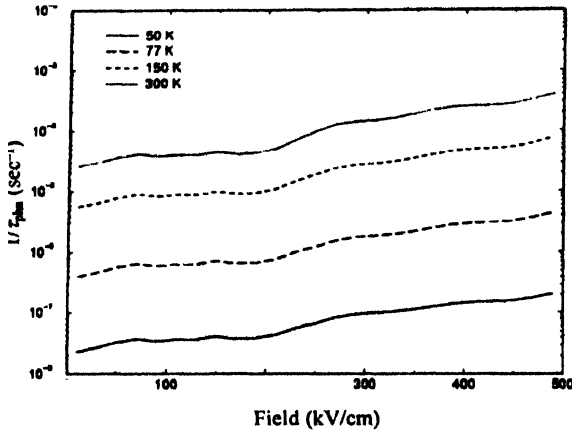


Figure 2. Phonon-assisted electron escape rate as a function of electric field for various temperatures, solid line :  $T = 50$  K, dashed line :  $T = 77$  K, long-dashed line :  $T = 150$  K and dotted line :  $T = 200$  K.

### 3. Dark current and photocurrent

#### 3.1. Dark current :

Under the applied bias the source current passes to the drain via the quantum well and then returns to the source by the closed circuit. In the steady-state condition the source current is the same so that the dark current is governed by the emitted current from the well by the electric field. Therefore the strength of the dark current depends on the two-dimensional carrier density ( $n_{2d}$ ) inside the well. The total current density is the combination of the tunneling current density and thermionic current  $J_{th}$

$$J_{dark} = en_{2d} \left\langle \frac{1}{\tau} \right\rangle + J_{th}, \quad (28)$$

where the total escape rate is expressed as the sum of two processes  $\langle 1/\tau \rangle = \langle 1/\tau_{th} \rangle + \langle 1/\tau_{ph} \rangle$ .

The thermionic emission has an important contribution to the tunneling process of electrons in the quantum well. The charge density outside the quantum well due to the thermal distribution is given by

$$n_{th} = \frac{(2m_B^*)^{3/2}}{2\pi^2\hbar^3} \int_0^\infty dE^- \frac{E^{1/2}}{\exp\left(\frac{E+V_0-\mu_F}{k_B T}\right) + 1} \quad (29)$$

where  $V_0$  is the barrier height and  $\mu_F$  is the chemical potential which is nearly temperature independent. The thermionic current density is given by [11]

$$J_{th} = en_{th}v_d, \quad (30)$$

where  $v_d$  is the drift velocity. The expression for  $v_d$  in the bulk GaAs [11],

$$v_d = \mu F / [1 + (\mu F / v_s)^\alpha]^{1/2}, \quad (31)$$

where  $\mu$  is the low-field mobility with value  $8000 \text{ cm}^2 \text{ V}^{-1} \text{ s}^{-1}$ ,  $v_s$  is the saturation velocity. Both  $\alpha$  and  $v_s$  are treated as two empirical parameters with values 2.7 and  $2 \times 10^7 \text{ cm/sec}$  respectively.

The dark current densities for various temperatures are shown in Figure 3.

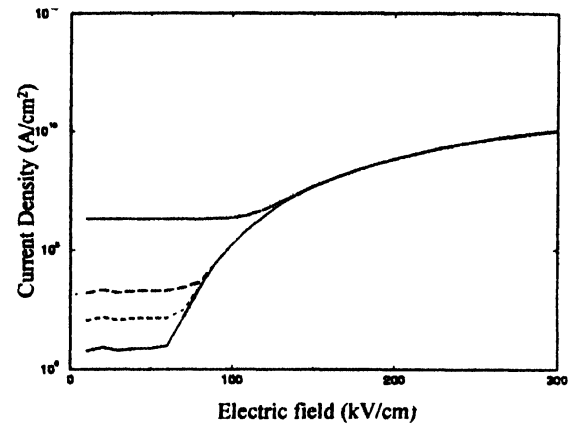


Figure 3. Dark current vs electric field for various temperatures. Notations are the same as in Figure 2.

As observed here, the direct tunneling current density is dominant in the high field region whereas the phonon-assisted tunneling current density and thermionic current density are dominant in the low field region.

#### 3.2. Photocurrent :

The photo-generated carriers at a given electric field produces photo-current. The photo-current is defined as [1]

$$I_p(F) = \frac{2eI_0}{\hbar\omega} \alpha(\hbar\omega)d, \quad (32)$$

where  $I_0$  is the power,  $\alpha(\hbar\omega)$  is the absorption coefficient and  $d$  is the width of the well. The absorption coefficient  $\alpha(\hbar\omega)$  due to the bound-to-continuum transition is calculated as [16]

$$\alpha(\hbar\omega) = \frac{\xi}{\hbar\omega} \int dE_{ip}(E_i) |O_{\beta}|^2 f(E_i) \times [1 - f(E_0 + \hbar\omega)], \quad (33)$$

$$\text{where } \xi = \frac{1}{137} \frac{1}{d} \frac{\pi}{n_r} \left( \frac{\hbar^2}{m_0} \right)^2. \quad (34)$$

The optical matrix element for an incident photon polarized in the  $z$  direction is given by

$$O_{fi} = \int dz \Psi_{E_f}^*(z) \frac{m_0}{m^*(z)} \frac{\partial}{\partial z} \Psi_{E_0}(z), \quad (35)$$

where  $E_f = E_0 + \hbar\omega - \hbar^2 k_f^2 / 2(1/m_B^* - 1/m_W^*)$ .

In Figure 4, we have compared photo-current calculated taking  $I_0 = 0.3$  W with the dark current at temperature 50 K.

As shown in Figure 4, the strength of the photo-current density is quite high compared to the dark current density. Therefore this well is suitable for fabricating photo-detectors.

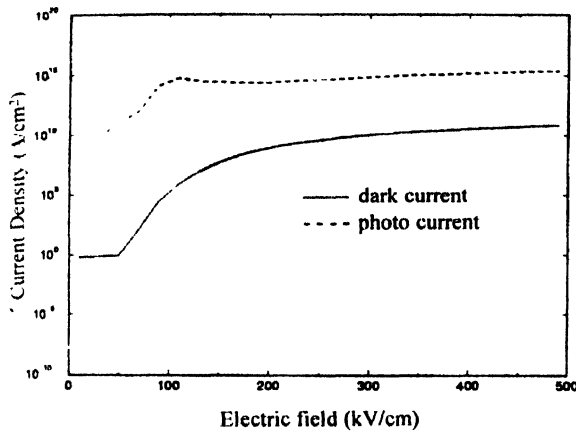


Figure 4. Photocurrent as a function of electric field with infrared power  $I_0$  0.3 W/cm<sup>2</sup>

#### 4. Conclusion

In the present work we have applied a new numerical method for finding quasi-bound energies and tunneling times under the applied electric field in a single rectangular quantum well fabricated from AlGaAs/GaAs heterojunction. The dark current is calculated using the field induced direct tunneling, LO phonon-assisted tunneling and thermionic emission

processes. The calculated photo-current shows that the dark current is not significant in this well so that this well is suitable for device applications.

#### Acknowledgment

One of the authors acknowledges the Council of Scientific and Industrial Research, India for awarding research associate position to carry out this work. The authors like to thank S G Mishra for valuable discussions.

#### References

- [1] K M Choi *The Physics of Quantum Well Infrared Photodetectors* (Singapore : World Scientific) (1997)
- [2] J P Loehr and M O Manasreh *Semiconductor Quantum Wells and Superlattices for Long-Wavelength Infrared Detectors* ed. M O Manasreh (New York : Artech House) (1993)
- [3] S Panda and B K Panda *Pramana* **56** 809 (2001)
- [4] S Panda, B K Panda and S Fung *J. Phys. Cond. Matter* **80** 1532 (2000)
- [5] B K Ridley *Electrons and Phonons in Semiconductor Multilayers* (Cambridge : Cambridge University Press) (1997)
- [6] P J Turley and S W Teitsworth *Phys. Rev.* **B44** 8181 (1991)
- [7] G D Mahan *Many-Particle Physics* (New York : Plenum) (1981)
- [8] R Ferreira and G Bastard *Phys. Rev.* **B40** 1074 (1989)
- [9] J Feldman, K Goossen, D Miller, A Fox, J Cunningham and W Jan *Appl. Phys. Lett.* **59** 66 (1991)
- [10] A F M Anwar and K R Lefebvre *Phys. Rev.* **B57** 4584 (1998)
- [11] D M T Kuo and Y-C Chang *Phys. Rev.* **B60** 15957 (1999)
- [12] S Panda *Quantum Confined State Effect and Optical Properties in Quantum Wells* (PhD Thesis, The University of Hong Kong) (1998)
- [13] A Hernandez-Cabrera, P Aceituno and H Cruz *J. Appl. Phys.* **78** 6147 (1995)
- [14] J Singh *Physics of Semiconductors and their Heterojunctions* (New York : McGraw-Hill) (1993)
- [15] P Harrison *Quantum Wells, Wires and Dots* (New York : John Wiley) (1999)
- [16] D M-T Kuo and Y-C Chang *J. Appl. Phys.* **87** 2936 (2000)